Catalysis Today 145 (2009) 204–212

Contents lists available at ScienceDirect

Catalysis Today

journal homepage: www.elsevier.com/locate/cattod

Recent progress in the use of in situ X-ray methods for the study of heterogeneous catalysts in packed-bed capillary reactors

Simon D.M. Jacques [a,b,*], Olivier Leynaud [a,b], Dmitry Strusevich [a,b], Paul Stukas [a,b], Paul Barnes [a,b], Gopinathan Sankar [a], Mike Sheehy [a], Matthew G. O'Brien [c], Ana Iglesias-Juez [c], Andrew M. Beale [c,**]

[a] Department of Chemistry, University College London, 20 Gordon Street, London WC1H 0AJ, United Kingdom
[b] Industrial Materials Group, Department of Crystallography, Birkbeck College, University of London, London WC1E 7HX, United Kingdom
[c] Inorganic Chemistry and Catalysis Group, Debye Institute for NanoMaterials Science, Utrecht University, Sorbonnelaan 16, 3584 CA Utrecht, The Netherlands

ARTICLE INFO

Article history:
Available online 21 March 2009

Keywords:
Heterogeneous Catalysis
In situ
Diffraction
EXAFS
Packed-bed reactors and synchrotron radiation

ABSTRACT

Synchrotron-based X-ray techniques, such as Diffraction and Absorption Spectroscopy (XAS), can be readily employed to study catalysts in action, thereby offering great potential for revealing the mechanism and behaviour of catalytic solids both during preparation and reaction. The continued advancement of X-ray generation and collection mean that it is now possible to obtain high quality data from catalysts under reaction conditions with second/sub-second time resolution. In this paper, we describe in detail a specific setup which can be used to obtain transmission in situ data. It is able to mimic industrial preparation/reaction environments and has been developed to such an extent that such measurements are now routine. To illustrate its applicability, we present time-resolved diffraction data obtained from an iron molybdate-based catalyst under pseudo industrial operating conditions revealing its bulk solid-state chemistry and stability, and further show how the catalyst behaviour changes as a function of the Fe/Mo ratio. We also illustrate the versatility of this setup in obtaining data using simultaneous multiple techniques (including non-X-ray-based methods, e.g. UV–vis) from an iron molybdate catalyst under methanol/air-flow. We conclude with a brief outlook towards the future, in which we identify new possibilities for studying catalysts in action which could yield insight into their preparation and behaviour.

1. Introduction

The study of catalysts under relevant reaction conditions enables the catalyst scientist to identify and understand the important steps in a catalyst's lifetime, e.g. the formation of active sites and reaction intermediate states, activation/deactivation and modes of regeneration. In reality the study of catalysts under true operando conditions is often too practically demanding to be feasible (e.g. large volume reactors, high pressures, etc.) leading to the need to make experimental compromises, resulting in the more generic term of 'in situ' studies. Critical to the acquiring of such insight has been the development of characterisation methods as well as the design and construction of appropriate in situ cells and reactor probes [1–14].

In situ synchrotron-based X-ray techniques, such as diffraction and XAS, are routinely used nowadays to investigate the chemistry of dynamically changing systems. Such studies have been made possible due to the nature of synchrotron X-rays (e.g. highly collimated, high brilliance, wide range of available photon energies) and the technologies associated with their detection. To date there have been a number of applications of synchrotron methods to the study of both catalyst preparation and operation, although perhaps not as many as one might expect. Thus such techniques remain seen as being far from routine. This may be because many researchers in the catalytic community are both unaware of what is now feasible (both technically and financially) and the relative ease of performing such studies, as well as the increased industrial accessibility to synchrotron technology (either directly or through academic collaboration). In this paper we aim to demonstrate the relative ease in which high quality scattering and spectroscopic data can be gleaned from catalysts undergoing reaction and the usefulness of such techniques in revealing and rationalising the chemistry involved. Much of the paper is dedicated to the practical considerations in the development and use of a plug-flow in situ capillary reactor, which, notably, has

* Corresponding author at: Department of Chemistry, University College London, 20 Gordon Street, London WC1H 0AJ, United Kingdom.
** Corresponding author.
E-mail addresses: s.jacques@bbk.ac.uk (Simon D.M. Jacques), a.m.beale@uu.nl (A.M. Beale).

0920-5861/$ – see front matter © 2009 Published by Elsevier B.V.
doi:10.1016/j.cattod.2009.02.012

been comparatively cheap to develop. We demonstrate the use of such apparatus with results taken from the study of iron molybdate, an important industrial catalyst used on the production of formaldehyde by direct oxidation of methanol. We also demonstrate its versatility for obtaining combined multiple technique data (using combined scattering and spectroscopic techniques) in order to investigate the catalyst in pseudo industrial operating conditions, and investigate the effect of Fe/Mo ratio to the activity and stability of the catalyst. We summarise with a look to the future of in situ X-ray studies which we believe offer great potential for further elucidating and understanding heterogeneous catalytic processes. We hope that this paper is of use to researchers in the field, both in academic and industrial institutions.

2. X-ray diffraction and scattering methods as a tool to probe the solid-state

Diffraction is widely employed in angle-dispersive reflection mode (sometimes referred to as powder diffraction) as a sample characterisation technique to identify polycrystalline compounds. However, the advent of more powerful and intense X-ray sources, coupled with the advances in data recording instrumentation, now allows for the collection of *medium-to-high quality* transmission diffraction signals on a second or sub-second time-scale. This approach is now being realised as a useful method for studying catalyst materials both during preparation and in action [15–21].

The diffraction signal is generated by the coherent elastic scattering from Bragg planes in well-structured crystals. The spacing and intensity of recorded diffraction maxima can be used to identify, quantify (typically to mass fractions as low as 1%) and monitor structural changes in crystalline materials. The amount of non-crystalline material can also be quantified by addition of a known mass of (benign) crystalline material, so called *spiking*. In addition the degree of crystallinity can be derived from the sharpness of the recorded maxima. Such information is useful for deciphering the mechanisms both in the formation of catalysts (mostly bulk materials) and indeed catalyst systems under reaction conditions.

It is also possible to probe systems which do not show long-range order using X-ray scattering techniques. Generally the techniques of diffraction and scattering can be differentiated as follows: diffraction being the elastic scattering of radiation from structures with long-range order, whereas scattering, which can be both elastic and inelastic, is typically employed to study samples that are organised on a smaller scale. Scattering is then also commonly delineated into two 'types': small angle X-ray scattering (SAXS) which probes structure in the nanometer to micrometer range (large length scale structures) by measuring scattering intensity at 2θ scattering angles close to 0° and wide angle X-ray scattering (WAXS), which concentrates on larger 2θ scattering angles. Often the two scattering techniques (SAXS/WAXS) are used in conjunction, particularly for studying the self-assembly processes during catalyst formation [22,23].

3. Probing the local environment of an atom type using EXAFS

X-ray absorption spectroscopy (XAS) has been successfully employed on numerous occasions to study catalysts under in situ conditions. The origin of this success can be attributed at least in some ways to the following two simple observations: (a) the technique can be employed to study both crystalline or amorphous materials where the element of interest can be as low as 0.1 weight %, and (b) the nature of the light source (highly penetrating and brilliant) in conjunction with the high availability of suitably robust X-ray transparent material avoids large compromises in cell design away from the operando 'philosophy'.

An X-ray absorption spectrum can be effectively divided into two parts: the X-ray absorption near edge structure (XANES), which concentrates on the region around an absorption edge (approximately 50 eV below and above) and extended X-ray fine structure (EXAFS), which is concerned with the analysis of data recorded some 100–1000 eV above the edge. Both aspects are sensitive to changes in a specific element's oxidation/coordination state, although it is also possible in some situations to obtain details on the absorbing element spin state.

Typically X-ray absorption spectroscopy can be measured in situ in two manners; transmission or fluorescence/emission. Normally the in situ time-resolved approach demands that a number of data must be collected in a short time period. Such data can normally be obtained with second to minute time resolution using quick XAS techniques (QEXAFS), which scan across and above an absorption edge by moving a monochromator incrementally and rapidly. Alternatively, an entire XAS spectra acquisition on heterogeneous catalyst samples can be obtained in the sub-second time regime (typically ms although experiments with a time resolution in the μs regime have recently been attempted) in energy dispersive mode (EDE), or via the use of fast sequential energy scanning QEXAFS monochromators [24,25]. With this propensity for rapid data acquisition, XAS has proven to be an extremely popular method to study both catalyst solid-state self-assembly processes and heterogeneous catalytic reactions, nowadays often in tandem with other scattering and spectroscopic techniques (e.g. SAXS/WAXS, IR, UV–vis, Raman, etc.) [22,26–30].

In order to achieve the time resolution required, both diffraction and EXAFS require a high spectral brilliance source, such as is available at a synchrotron. Whilst the rest of this article will focus principally on the benefits this can bring, it is worth mentioning at this stage some points of caution. Firstly that one should be aware that in some cases exposure to such X-rays can induce sample damage [31]. Secondly that, not surprisingly, the benefit of the higher time resolution has meant that more data can be collected. This coupled with the potential complexities of handling data derived from these techniques often leads to time-consuming analysis.

4. The suitability of small tube reactors for in situ studies

There are two considerations when designing sample cells and cell environments for in situ measurements: (a) that the setup and reaction conditions remains as close to being industrially relevant as possible and (b) that the design does not, or to the most limited sense, impinge on the quality of the data collected. However, often such designs make a compromise between these two ideals [13]. When considering measurements in transmission mode an important consideration is working at or near an *ideal sample path length*, i.e. the length of sample material/reactor wall through which the incident light must pass. This is dependent on the absorbing nature of the material under study and the wavelength(s) to be used, and also requires that the sample is uniformly 'transparent'. The ideal path length is calculated according to the stoichiometric approximation [32] from the component elements mass attenuation coefficients [33] (Figure S1, in electronic support information, shows the ideal path length as a function of wavelength for iron molybdate, a component in the Fe–Mo–O mixed oxide catalyst system). Clearly, even at high energies (e.g. 100 keV) there is still significant self-absorption. In this regard, cell designs in which the sample is mounted as a pressed pellet/wafer are well suited. However, there are two drawbacks associated with this type of cell design for studying gas-phase reactions. Firstly the diffusion of the reactants/products is impeded, and secondly, the shape of the catalyst sample results in there being a limited amount of space around which to perform additional comple-

mentary measurements. Owing to such restrictions we have focussed on using packed-bed capillary-tube reactors with a controlled particle size distribution, which resemble more closely the conditions/circumstances found industrially. The suitability of such reactors has already been demonstrated [14,34–37].

Capillaries and small diameter tubes, by their cylindrical nature, can support comparatively high pressures for small wall thicknesses, e.g. a standard borosilicate 0.5 mm diameter capillary with a wall thickness of 10 μm can withstand a pressure of 30–50 atm. Thin walls and small sample volumes allow fast transmission of heat and allow for design of finely controllable heating environments. Such volumes obviously require less sample which can have advantages from a synthesis view point. It follows that small catalyst volumes require relatively small reagent volumes, which have safety-related benefits when working with flammables/explosive reagents. Glass-walled capillary tubes have the additional advantage over capillary tubes constructed of high X-ray transmission materials such as beryllium [32] and boronitride in that the sample is visible; this helps when loading the sample (to know for instance, that the sample is evenly distributed) and importantly allows for additional measurements to be made using visible/near-visible light such as UV/vis, Raman, etc. Additionally, it is relatively easy to recover studied samples (perhaps for further analysis by, e.g. TEM to elucidate deactivation phenomena) from such sample cells. However, it should be noted at this stage that the use of mounted capillaries is not without its disadvantages. For example, it can be difficult to load samples, especially when using $Ø \leq 0.5$ mm capillaries; the symbol Ø indicates diameter. The sample should be uniformly loaded and of sufficient thickness to ensure a good quality signal whilst, at the same time, allowing for sufficient gas permeation without a too significant pressure drop across it. A standard protocol is used to prepare the sample for investigation in which it is first pressed into a pellet (care must be taken not to over press the sample which would lead to damage, manifesting as stress-broadening) before it is crushed and sieved to the required fraction range. This fraction is then packed into the reactor using a combination of thin wire ($Ø < 0.3$ mm) and gentle tapping on the side or the use of a corrugated edge (e.g. a coin or small screw) to coax material to drop down into the tube. Either side of the sample are placed two quartz wool plugs (to prevent sample blow out). The end of the capillary is then scored with a glass scorer and broken off. We use Glasinstrumentumachermeister Wolfgang Muller capillaries that are typically 80 mm long inclusive of a typical bulb length of 10 mm. At this stage we slide a PTFE ferrel over the capillary and glue it into position. The capillary and ferrel is mounted in a *gas stub*, a check is carried out for gas flow, and finally the capillary/gas stub is aligned with respect to the beam and the experiments performed.

A second problem concerns the sensitivity of the data to the experimental setup. In Fig. 1, we show the effects of catalyst sieve fraction size and beam position on the quality of the transmission diffraction and XAFS data obtained on $Cu/Zn/Al_2O_3$ catalysts. As can be seen from the figure, these parameters have a significant influence on the data. These differences are caused essentially by variations in the diffracting/absorption volume (and for XAFS by the sample uniformity) and affect more significantly the XAFS data than the diffraction. Perhaps most interesting is the effect of particle size. The desired lower particle packing efficiency associated with larger catalyst particles results in a significant reduction in the overall quality of the XAFS data (due to a smaller absorption volume) and its amplitude since it is akin to a severe 'pin-hole' effect. This effect is extreme in the case of large particles, becoming increasingly less so as the particle size decreases and has obvious implications when trying to extract EXAFS information (particularly with respect to coordination number). Differences in the quality of the diffraction data are also noticeable. For larger

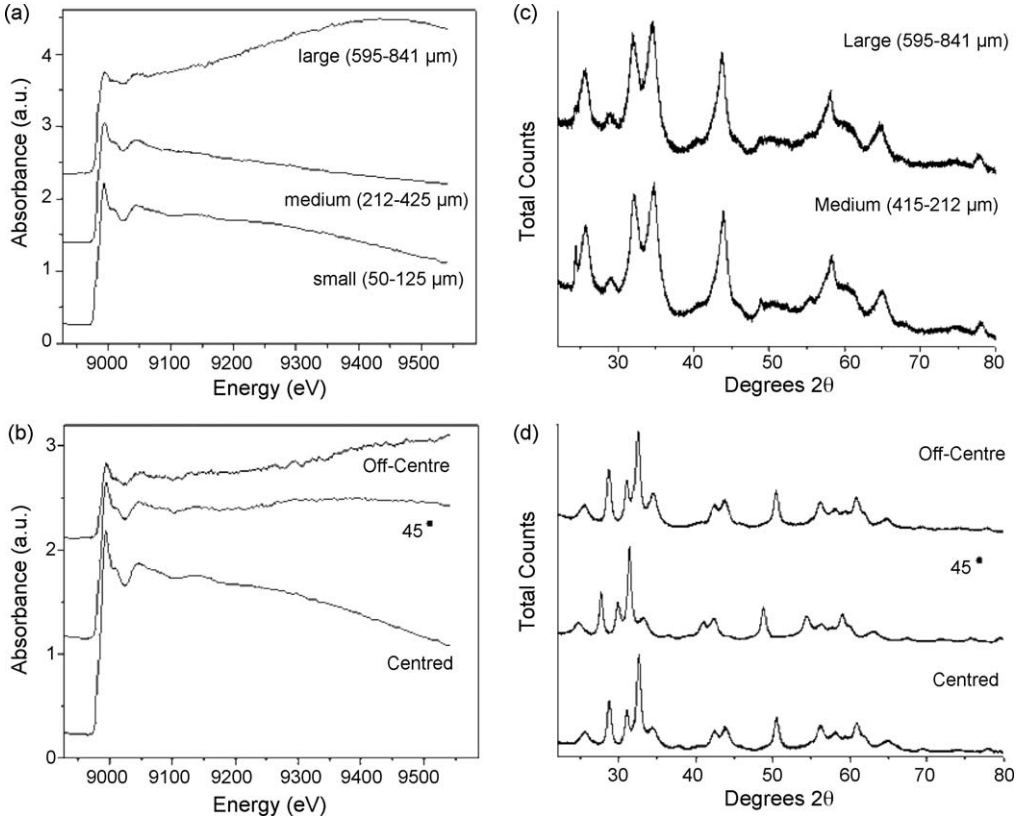

Fig. 1. Comparative XAFS data ((a) and (b)) recorded at the Cu K-edge (8.789 keV) and WAXS data ((c) and (d)) recorded at 1.398 Å illustrating the influence of beam position and catalyst sieve fraction size on data quality.

sized particles a lower number of counts are recorded on the detector thus making it difficult to resolve weakly diffracting peaks unless longer count times are employed. Slight variations in peak intensity can also be seen which are most probably due to preferred orientation.

The influence of the beam position/sample angle on the differences in the XAFS and diffraction data can be explained to a large extent (as mentioned above) in terms of the variation in the diffracting/absorption volume element. However, the shift in the XRD peak positions occurs due to the change in sample-to-detector distance.

5. Required components for in situ studies and our setup

Performing in situ experiments requires some or all of the following components: gas delivery system, vapour pressure control system, heating and temperature control systems (furnace), exhaust gas analysis and the possibility to include additional measurement probes. In building apparatus for in situ experiments at synchrotron radiation sources it is strongly desired that the apparatus is safe, is easy to use, is both portable and durable, and is not cost prohibitive. Here we describe the components that we have developed for our in situ studies (a typical setup may include the components indicated schematically in Figure S2). Similar types of setup have been previously described (e.g. [16,34,38–40]) and bespoke setups for particular synchrotron stations have been developed [41,42].

Gas delivery, was carried out using Bronkhorst F201CV mass flow controllers (MFC) with a capability to deliver an output flow rate of 0–50 ml/min (with a control interval of 2% of the maximum). Typically 3 types of gases were selected for any one experiment: a diluent inert gas (e.g. nitrogen, argon or helium), an oxidant (oxygen typically 5% in an inert gas) and a reductant (hydrogen also 5%). These devices are controlled electronically using a 0–5 V continuous signal to deliver a flow of 0–50 ml/min at a working inflow range of 1–3 atm. The input voltage is regulated via a MFC control box, which possesses also the capacity to receive a bespoke 5 V TTL external trigger (initiated by the experimental acquisition software; most synchrotron stations have 5 V triggers such that events can be triggered to coincide with data acquisition events), that would allow for switching between gases (at set desired delivery rates). MFC's are then supplied from gas cylinders of pure or pre-mixed gases via, preferably, stainless steel gas tubing since Teflon type tubing is known to be pervious to small atmospheric gas molecules such as oxygen. Occasionally oxygen and water scrubbers are attached to the inlet lines to ensure the reactant gases are of the best purity. We observe also that it is important to have double-stage regulators for bottles to avoid variations in the MFC inflow gas pressure.

In the cases where the reactant at room temperature is a solvent (e.g. methanol used in selective oxidation experiments) yet the reaction is carried out in the gas phase, a bubbler is employed through which a *carrier gas* is pushed through by one of the MFCs. Cleary this can only work if the vapour pressure of the solvent in question is sufficiently high enough to obtain the required amount of reactant for the catalytic process under study. Furthermore the bubbler should possess a significantly large enough 'dead volume' above the reservoir of liquid reactant in order to allow for good mixing with the incoming carrier gas resulting in a steady supply of reactant in the gas stream. Alternatively, the solvent can be introduced via a loaded syringe/syringe pump arrangement which allows for a much more controlled introduction. When using a bubbler it is necessary to heat it in order to obtain the required vapour pressure and therefore required amount of reactant. However, this also means that not only the reservoir of solvent needs to be heated but also the transfer gas lines (preferably both into (for preheating) and out of the bubbler) need to be maintained at a similar temperature in order to avoid condensation. Here, the pipe that delivers the gas from the bubbler to the sample cell is held at constant temperature by being bathed (by virtue of a larger diameter pipe) in circulating heated oil which by conduction heats the metal components. This method is reliable for maintaining vapour pressure. It has been our experience that maintaining vapour pressure through the use of heating tape and insulation has been difficult to achieve, since it is difficult to eliminate every cold spot by this method.

Typically our in situ experiments have been conducted with 0.5–1 mm diameter capillaries. The use of capillaries requires a gas tight seal. This is achieved by use of a PTFE ferrule which is slid over the capillary and glued against the capillary bulb (using superglue). During the experiments the PTFE ferrule is sufficiently far from the heating zone that it is not deformed by heat. The ferrule is secured to the *gas stub* via a standard Swagelok nut, see the schematic and photographs in Fig. 2. The gas stub consists of a rotating seal (suitable for work up to 4 atm, above this a gas stub without rotating seal is used) and quick fit pipe (gas inlet) connector. The stub can be mounted into a standard 6 mm goniometer such that sample alignment can be achieved. Although we have a working and tested rotating seal we have not successfully used this with a standard motor driven goniometer as spinning requires considerable torque (spinning the capillary in powder diffraction is desirable, as it averages crystallite orientations, but not necessarily a requirement). In this cell, the capillary is not sealed on the output side, though many cell designs incorporate a seal, e.g. [14].

Heating is achieved in one of two manners; radiative heating furnaces or hot air blowers. A general type bespoke furnace (here referred to as the mark 1 furnace) used with 1D detector systems (such as the RAPID-2 or delay-line curved INEL detectors) is shown in Fig. 3. The heating element consists of kanthal wire of 1 m in length (with resistivity of 11.1 Ω m^{-1} wound into a coil) supported on a pyrophyllite ceramic; the latter material chosen for its thermal and machinability properties. Coiling the filament wire and threading it through the ceramic ensures that there is sufficient length to achieve resistance of at least 10 Ω. This also serves to better concentrate the heat around the capillary and results in a compact heater cage design. The heating cage is insulated from the aluminium body by glass wool, ceramic plates and fire-board. The body has been machined with a 10 mm incident X-ray window, and a 10 mm wide 120° exit X-ray window, both of which are kapton covered; the exit window is air-cooled. The aluminium body is maintained at a safe handling temperature with external water-cooling circulating via wrapped copper piping. The furnace is controlled by the commercially available Eurotherm 2204 furnace controller fitted into a specially designed power supply box. The furnace/controller is capable of running heating/cooling programs with ramp rates of up to 30 °C min^{-1} up to temperatures of ~950 °C, beyond which there is a risk of the heating wire burning out. The mark 2 furnace (shown in Figure S3), has a slimmer body such that a standard capillary will traverse the body in order that the outflow end of the capillary is easily accessible and that the product gasses can be easily collected. A drawback of this furnace is the open filament heater cage, which makes it incompatible with the measurement of UV/vis data due to its signal being overwhelmed by black body radiation. A second 'shielded filament' heater cage was designed to overcome this problem; with this cage the furnace is less responsive (~5 °C min^{-1}) and can only operate up to 650 °C.

We have also employed heater guns as an alternative heating method. The use of guns has the primary advantage that they give greater sample access space, and as such are suitable for use with 2D detectors with additional probes (a typical setup is shown in Figure S4).

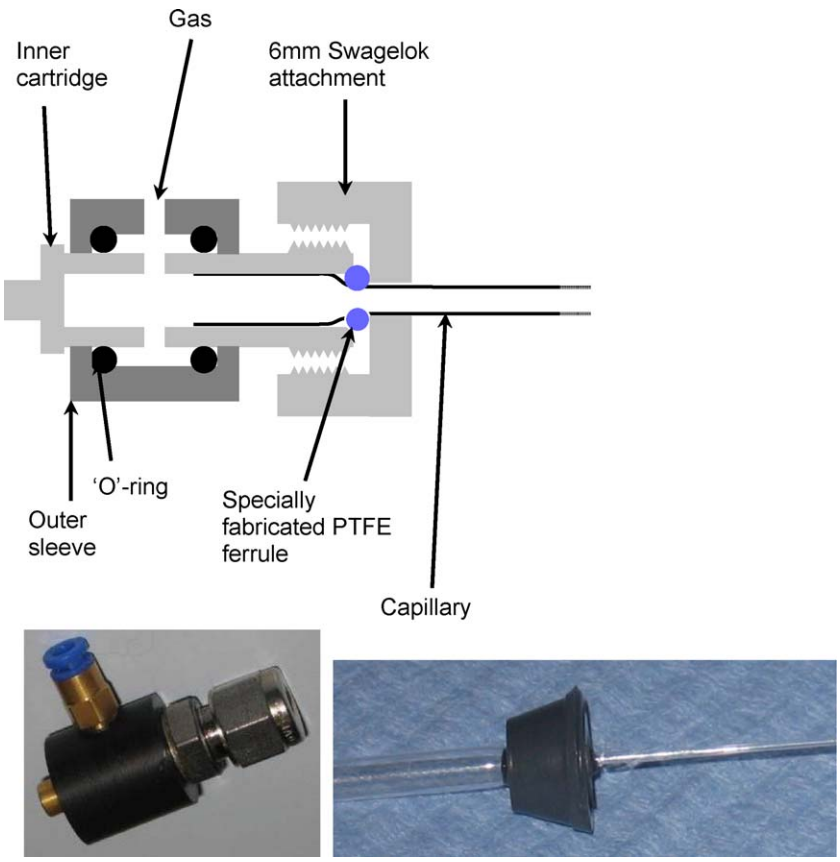

Fig. 2. *Top* schematic of capillary in gas stub. *Bottom left* photograph of gas stub (the gas inlet is via a quick push fit pipe connector suitable for 4 mm ∅ pipe). *Bottom right* capillary glued into PTFE ferrule.

6. Selected results

The studies presented below aim to illustrate the suitability of small tube reactors for in situ studies. The results represent work in progress on rationalising the behaviour of the iron molybdate catalyst ($Fe_2(MoO_4)_3/MoO_3$), used in the industrial production of formaldehyde by direct oxidation of methanol (MeOH).

7. Probing solid-state redox behaviour

The importance of the solid-state chemistry between the respective crystalline phases ($Fe_2(MoO_4)_3$, β-$FeMoO_4$ and MoO_3) of the iron molybdate catalyst was studied using a rapid powder diffraction setup, which allows for the collection of refinable full-pattern data in 1 s [21]. This allowed us to follow the time-sequence of interplay between these component phases and, in particular, how differences in the rates of solid–solid reactions in 5% H_2 or O_2 were important for maintaining the catalyst's stability.

Fig. 4 shows selected results from the reduction–oxidation cycling of the iron molybdate catalyst at 472 °C. Fig. 4(a) shows a typical diffraction pattern from the experiment. The three crystalline phases ($Fe_2(MoO_4)_3$ (high temperature form), MoO_3, and β-$FeMoO_4$) were clearly identifiable. No peak remains unexplained and the main intensity mismatch is attributed to

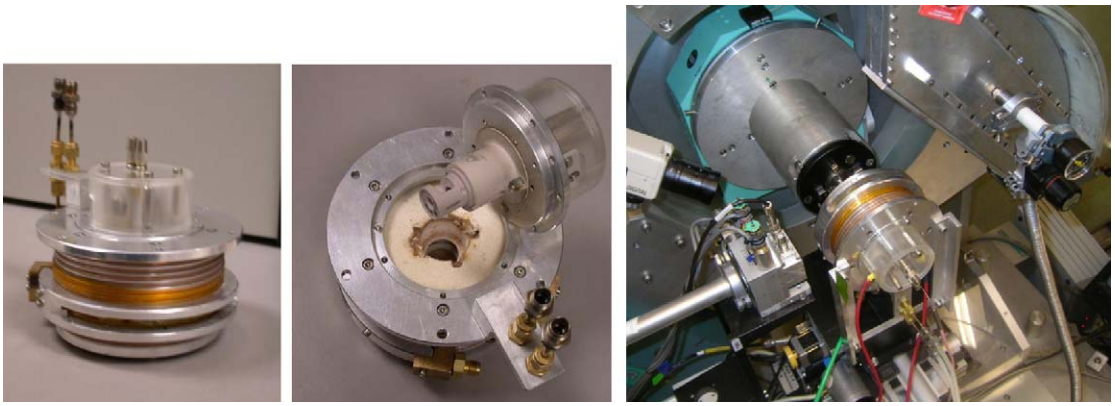

Fig. 3. Mark 1 furnace, *left* showing the X-ray exit window and the water-cooling jacket; *centre* heater cage and the internal insulation, water and air cooling inlet and *right* mounted on station 6.2, SRS. The furnace has body dimensions of ∅ = 150 mm and height 80 mm with an X-ray entrance exit window of 10 mm × 120°. The pyrophyllite heater cage has dimensions 25 mm length, external barrel ∅ = 20 mm, internal barrel ∅ = 8 mm, with an X-ray entrance window of 10 mm × 2 mm and exit window of 10 mm × 120°. A standard capillary will not traverse the body of the Mark 1 furnace; a mass spectrometry line can be inserted at the capillary outlet, but with difficulty.

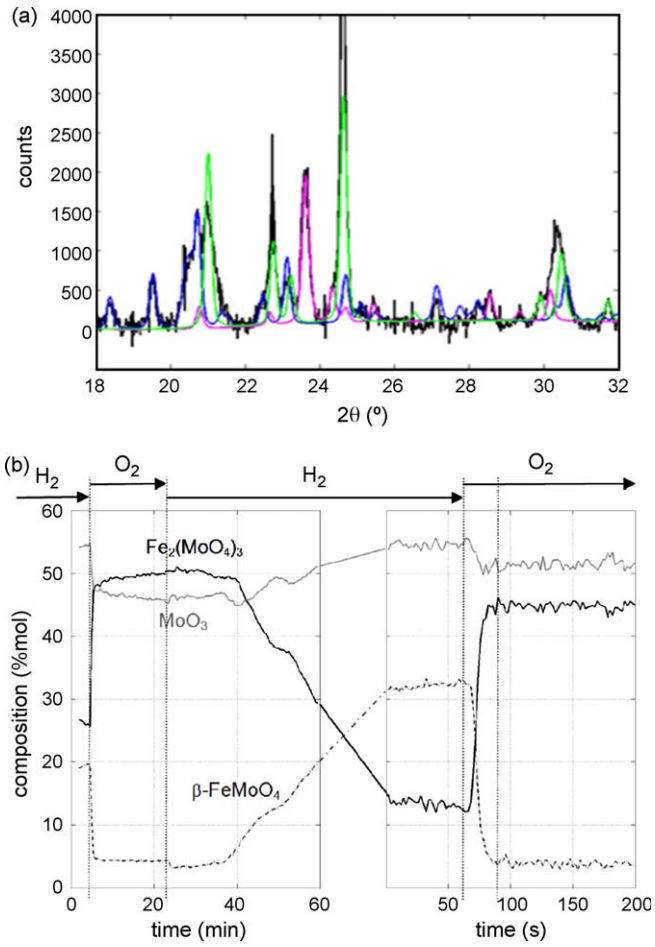

Fig. 4. (a) A magnified section of part (2θ = 18–32°) of the background-subtracted powder diffraction pattern from the catalyst during an early reduction stage against the three component fitted phases: (- - -) $Fe_2(MoO_4)_3$, (- - -) β-$FeMoO_4$, (- - -) MoO_3. (b) Phase composition (% mol weight fractions) of $Fe_2(MoO_4)_3$ (solid black line), β-$FeMoO_4$ (dashed gray line) and MoO_3 (solid light gray line) as derived by multiphase quantitative Rietveld fitting to the data in (b).

the MoO_3 phase (due to the preferred orientation of its lamellar structure). The data were refined independently, using the Celref [43] and Fullprof [44] packages to obtain the respective phase weight fractions and intensities proportional to those for the respective structures. Fig. 4(b) shows that $Fe_2(MoO_4)_3$ forms β-$FeMoO_4$ (and MoO_3, see Eq. (1)) in the presence of H_2 but reforms again in the presence of O_2 (Eq. (2)). However, as can be seen in Fig. 4(c), reduction appeared to be a much slower process than the reverse re-oxidation reaction; the rapidity of which was revealed during studies performed on a 2-s time interval basis and shows that the oxidation reactions are virtually completed within 15 s (it is worth noting at this stage that this solid-state reaction between β-$FeMoO_4$ and MoO_3 occurred at a rate never seen before in nature under such mild conditions). In comparison reduction was much more gradual, taking place over a number of minutes.

$$H_2 + Fe_2(MoO_4)_3 \rightarrow 2(\beta\text{-}FeMoO_4) + MoO_3 + H_2O \quad (1)$$

$$2(\beta\text{-}FeMoO_4) + MoO_3 + \tfrac{1}{2}O_2 \rightarrow Fe_2(MoO_4)_3 \quad (2)$$

Further investigative redox studies were performed as a function of molybdenum concentration in order to determine further its role in the solid-state chemistry of this catalyst. Three samples were compared in which the Mo:Fe ratio varied from 1.5:1 ($Fe_2(MoO_4)_3$) up until 3:1. Shown in Fig. 5(a) is a plot of the data for the Mo:Fe 3:1 sample during both reduction and oxidation cycling. The phase composition plot in Fig. 5(b) details the rate of β-$FeMoO_4$ formation (reduction), where it is clear that the rate of reduction is much quicker for the sample containing more molybdenum. Although not shown here, the rate of re-oxidation was also found to be fastest for the 3:1 sample. Peak shape profiling revealed that at the point before reduction began, the peak widths for the $Fe_2(MoO_4)_3$ phase were very comparable, thereby eliminating the possibility that such a difference originates from the difference in particle size.

From these studies it was possible to rationalise the behaviour of the catalytic system as follows. In a 5% H_2/Ar atmosphere the $Fe_2(MoO_4)_3$ phase in the mixed Fe-Mo-O catalyst undergoes a slow reduction according to Eq. (1) but undergoes rapid regeneration in 5% O_2/Ar according to Eq. (2). The observation appeared contrary to the previous work [45] in which it was stated that reduction of $Fe_2(MoO_4)_3$ is much easier than oxidation of β-$FeMoO_4$. Reduction does however occur more quickly with higher molybdenum loadings, although it is not clear why. This might be due to the higher loaded sample possessing a larger surface area, or else may possibly be due to some sort of promotion effect by the MoO_3, or a partial substitution of Fe^{3+} in the $Fe_2(MoO_4)_3$ structure. Since it has been well documented that $Fe_2(MoO_4)_3$ is active for MeOH conversion [46] this difference in reactivity could be critical for maintaining phase stability and therefore the catalyst activity. This and the absence of any additional phases suggested that reaction (2) proceeds so quickly that other solid-state side reactions leading to deactivation (3) cannot occur. This observation, coupled the increased rate of re-oxidation with increasing molybdenum concentration, implies that adding an excess of MoO_3 in the as prepared catalyst is beneficial for maintaining the stability of the active phase as well as for replenishing any sublimed molybdenum. This then appears to be a key step in understanding the

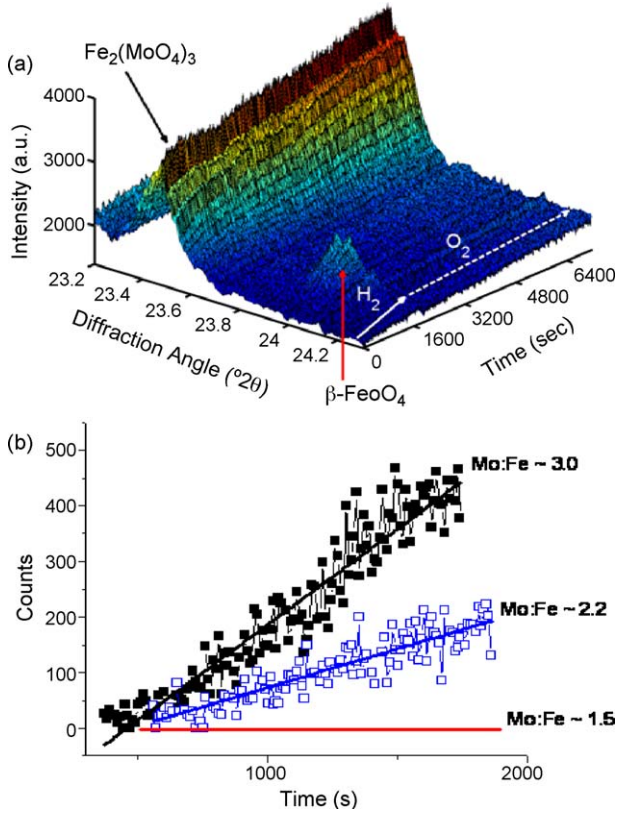

Fig. 5. (a) Time-resolved plot recorded from the $Fe_2(MoO_4)_3/MoO_3$ (Mo:Fe ~ 3.0) during H_2/O_2 cycles. (b) Plot of relative formation rates of β-$FeMoO_4$ as a function of [Mo].

catalyst's longevity. Thus we propose a new 'role' for excess molybdenum in the catalyst formulation.

$$2(\beta\text{-}FeMoO_4) + \tfrac{1}{2}O_2 \rightarrow Fe_2O_3 + 2MoO_3 \quad (3)$$

8. Activity in MeOH

H_2 was used as the reductant in the previous studies since it is known that polar solvents such as MeOH, formaldehyde or water can cause molybdenum volatilisation. Such an effect could have a negative influence on the rate(s) of solid-state reaction and was therefore avoided. However, it is far more relevant to compare catalyst activity/behaviour using MeOH and therefore MeOH and O_2 cycling experiments were performed. In these experiments, MeOH was passed over a series of catalysts during temperature ramping in an attempt to determine the effect of increased molybdenum loadings on the light-off temperature. Our rationale was that under typical aerobic conditions, little variation in the light off temperature would be observed when compared to anaerobic conditions, where differing molybdenum loadings (ranging from Mo:Fe = 1.5 to 3.0) may influence significantly oxygen transfer through the bulk. Such differences then may lead us to further understanding of the role of excess molybdenum in the catalyst formulation.

Fig. 6, contains a stack plot of the data recorded for a Mo:Fe ~ 3.0 system. The catalyst, somewhat unexpectedly, underwent a number of changes during temperature ramping. The peaks corresponding to both the $Fe_2(MoO_4)_3$ and MoO_3 phases were observed to gradually disappear (via the appearance of MoO_2 and possibly β-$FeMoO_4$) with increasing temperature so that on reaching the end of the temperature ramp (440 °C) only weak reflections at 32.79°, 47.90° and 59.11° 2θ remained against a broad (increased) background. The remaining Bragg peaks were too weak to assign definitively to a particular crystalline phase, although it was possible to rule out the presence of any known iron molybdate or molybdenum oxide. Based on pattern matching, the most likely phase assignment is MoC, although the increased background suggests that amorphous phase(s) might also be present. On switching back to air however, the MoC phase was observed to first disappear before the mixed $Fe_2(MoO_4)_3/MoO_3$ phase reformed (also via MoO_2) in an identical ratio to that seen at the start of the reaction ($FeMo/MoO_3$, 1:1). The peaks were however slightly sharper, suggesting that sintering had occurred. Similar behaviour was observed for all catalysts studied and further studies are in progress in order to understand why this occurs.

9. In situ multi-technique study

The simplicity of the capillary setup means that it can be easily transferred to other beamlines to perform complementary measurements. Furthermore its 'open' design allows for the performing multiple measurements at the same time, potentially enabling greater insight into the catalyst's behaviour. The multi-technique approach has the obvious advantage that it allows the experimenter to capture information under one set of experimental conditions, i.e. they do not need to be recreated for each individual measuring technique. As an example, Fig. 7 shows WAXS/XAFS/UV–vis and mass spectrometry data recorded during temperature ramping in MeOH, although to the slightly lower temperature of 350 °C. As observed previously (Fig. 6), heating in MeOH led first to the disappearance of $Fe_2(MoO_4)_3$ and MoO_3 and the gradual formation of MoO_2 along with diffraction amorphous material. Interestingly, and in contrast to the previous study, no MoC phase was observed to form which is probably due to

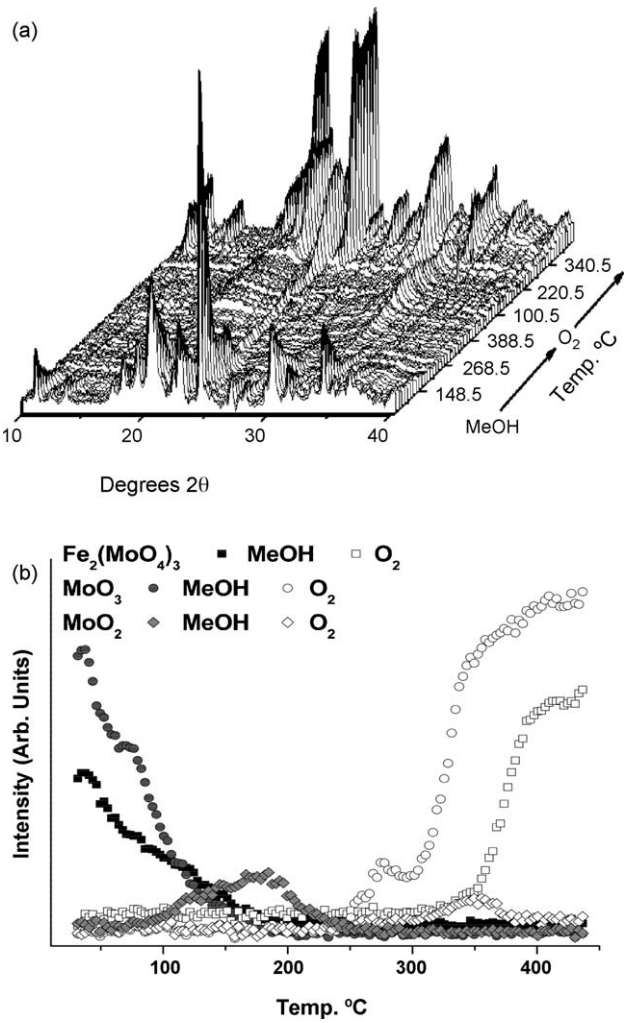

Fig. 6. (a) Time-resolved stack plot recorded for the $Fe_2(MoO_4)_3/MoO_3$ (Mo:Fe ~ 3.0) during MeOH/O_2 gas switching during temperature ramping (to 440 °C). (b) Graph detailing the evolution of crystalline phases (for clarity the evolution/disappearance of the small amount of MoC phase is not shown) as a function of temperature and atmosphere. Closed symbols correspond to the phase evolution under MeOH and open symbols under O_2. Note actual intensities were used.

differences in the temperature/heating method. The changes in the WAXS were accompanied, on reaching reaction temperature, by a shift in the Mo K-edge energy to lower energies and also a decrease in the intensity of the pre-edge feature (at 19999.95 eV) [20,47]. Both changes are consistent with a reduction in the Mo oxidation state from 6+ to 4+ and therefore the data correlated well with the observed formation of MoO_2. A stack plot of the accompanying UV–vis data revealed that an increase in absorption occurs on reaching 160 °C (before changes were observed in the WAXS and XANES data) and continues to increase for the remainder of the experiment until essentially the sample is so dark that no UV–vis signal can be recorded. This change in color is consistent with the appearance of black MoO_2. The observation that the changes in the UV–vis data occurred before those observed in the WAXS and XAFS indicates that reduction of the catalyst occurs to some extent (most likely on or near the surface) prior to changes in the bulk. The mass spectrometry traces for m/z = 18 (H_2O), m/z = 30 (HCHO) and m/z = 31 (CH_3O^-) suggested that small amounts of formaldehyde began to form at temperatures ca. 270 °C, before peaking 7 min after reaching isothermal. Peak formaldehyde activity coincided with the presence in the sample of both MoO_3 and MoO_2, but a lack of $Fe_2(MoO_4)_3$. Later however, increasing amounts of MoO_2

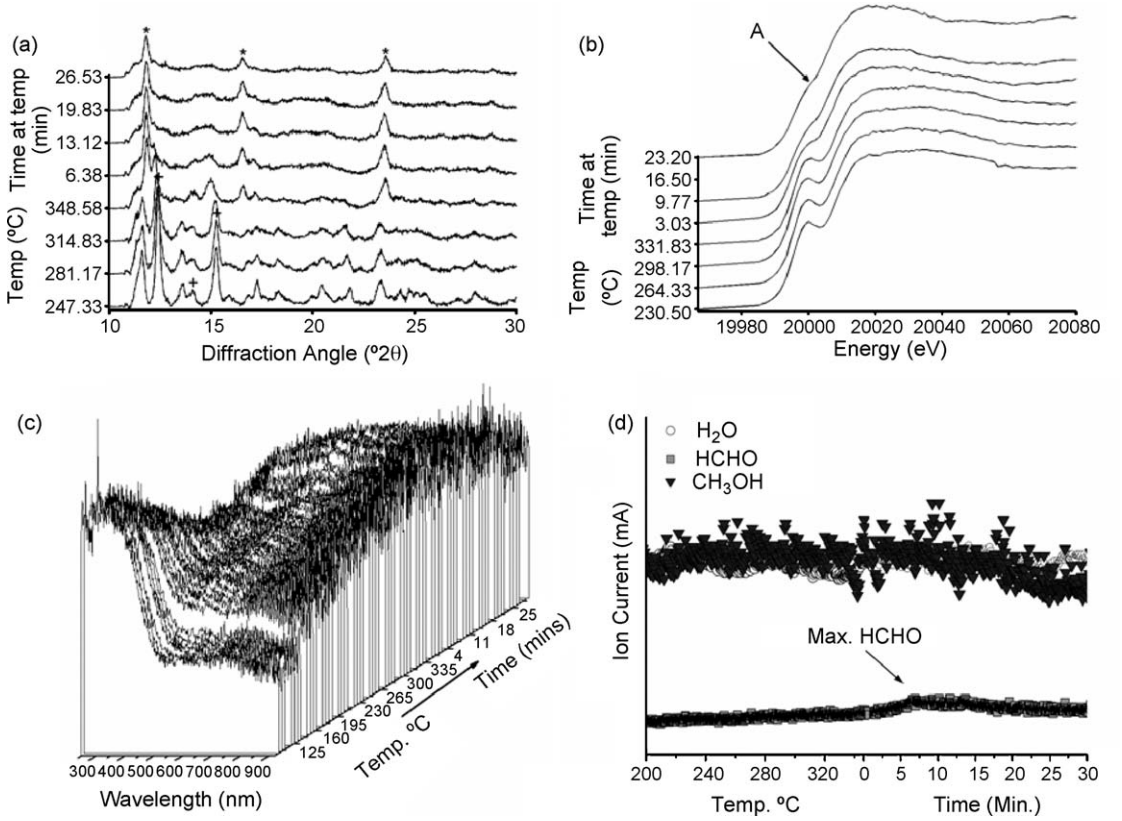

Fig. 7. Combined in situ WAXS (a), Mo K-edge XANES (b), UV–vis (c) and mass spectrometry data (d) recorded during the heating of a $Fe_2(MoO_4)_3/MoO_3$ catalyst under MeOH/He. The peaks marked * and + in (a) correspond to peaks due to MoO_2 and MoO_3 respectively. Feature 'A' in (b) highlights the 1s–4d peak at the Mo K-edge. The shift to lower energies and decrease in intensity of the pre-edge feature are consistent with oxidation state change from 6+ to 4+.

coincided with a decrease in the amount of formaldehyde, therefore suggesting that under these conditions, MoO_3 is the most selective/active for this reaction.

10. Summary and future perspectives

The examples discussed above serve mainly to illustrate the possibilities of applying X-ray-based methods for the study of packed-bed capillary reactors under reaction conditions. A number of examples exist in the literature, where such methods have been successfully employed and new insight has been obtained. Until recently, studies of this kind, were almost certainly the preserve of research groups that invested considerable time and effort in such endeavours. The fact that these studies were not more widely accessible was due, amongst other things, to the difficulties in gaining access to synchrotron time, the complexity and expense associated with building the appropriate apparatus, and the difficulties associated with analysing the data. However, greater availability of beamlines (and synchrotrons in general), decreasing costs of equipment, and the development of more user-friendly software, mean that such 'problems' almost cease to exist and such measurements should now be considered fairly routine. Continuing technological developments are yielding further/deeper insights into 'catalysts in action'. For example, increased brilliance and better performing detectors allow for better time resolution and the possibility to study/identify the 'active sites' in materials with low concentrations [48]; the availability of higher energy/shorter wavelength photons permits the collection of both elastically and inelastically scattered signals [49], even through relatively thick sample containment environments. Another area of exciting development is the *imaging* of catalysts in action using X-ray-based methods, including those methods described in this paper. As an example, diffraction has been used to directly image the distribution and composition of metal oxide species in catalyst bodies [50]. Imaging dynamic systems is also possible, e.g. time-resolved 1D diffraction traverses of in operando catalyst beds have been carried out showing that there is significant process variability along the length of the catalyst bed. Most recently, 2D time-resolved X-ray absorption [36,37] and diffraction has been undertaken to study evolving catalytic systems. Such developments show that in situ/in operando X-ray methods offer great potential for studying catalytic systems. We hope that these methods stimulate and enthuse the interest of the catalyst scientist.

Acknowledgements

The authors kindly acknowledge the following people for the stated contributions: Mr. Martin Vickers for the construction of the furnace power-supply box, Drs. Wim Bras and Sergey Nikitenko for help in the setup/data collection on DUBBLE, ESRF, Dr Chris Martin for his help on station 6.2, SRS and Prof. Bert Weckhuysen for his scientific contributions and insight. Also, the authors wish to acknowledge EPSRC for funding through a Portfolio grant and from NWO-CW, for a VENI award (AMB).

Appendix A. Supplementary data

Supplementary data associated with this article can be found, in the online version, at doi:10.1016/j.cattod.2009.02.012.

References

[1] J.F. Haw (Ed.), In Situ Spectroscopy in Heterogeneous Catalysis, Wiley–VCH, Weinheim, 2002.

[2] B.M. Weckhuysen (Ed.), In Situ Spectroscopy of Catalysts, American Scientific Publishers, Stevenson, 2004.
[3] M. Hunger (Ed.), J. Weitkamp Angew. Chem. Int. Ed. 40 (2001) 2954.
[4] B.S. Clausen, H. Topsoe, R. Frahm, Adv. Catal. 42 (1998) 315.
[5] B.M. Weckhuysen, Chem. Commun. (2002) 97.
[6] M.A. Banares, Catal. Today 100 (2005) 71.
[7] I.E. Wachs, Top. Catal. 8 (1999) 57.
[8] A. Brückner, Catal. Rev. Sci. Eng. 45 (2003) 97.
[9] C. Prestipino, F. Bonino, S. Usseglio, A. Damin, A. Tasso, M.G. Clerici, S. Bordiga, F. D'Acapito, A. Zecchina, C. Lamberti, Chem. Phys. Chem. 5 (2004) 1799.
[10] M. Tada, Y. Iwasawa, Ann. Rev. Mater. Res. 35 (2005) 397.
[11] J. Evans, A. Puig-Molina, M. Tromp, MRS Bull. 32 (2007) 1038.
[12] J.D. Grunwaldt, R. Wandeler, A. Baiker, Catal. Rev. Sci. Eng. 45 (2003) 1.
[13] J.D. Grunwaldt, M. Caravati, S. Hannemann, A. Baiker, Phys. Chem. Chem. Phys. 6 (2004) 3037.
[14] P.J. Chupas, K.W. Chapman, C. Kurtz, J.C. Hanson, P.L. Lee, C.P. Grey, J. Appl. Crystallogr. 41 (2008) 822.
[15] H. Jung, W.J. Thomson, J. Catal. 134 (2) (1992) 654.
[16] P.J. Chupas, M.F. Ciraolo, J.C. Hanson, C.P. Grey, J. Am. Chem. Soc. 123 (2001) 1694.
[17] L. O'Mahony, D. Sutton, B.K. Hodnett, Catal. Today 91–92 (2004) 185.
[18] J.S.J. Hargreaves, Cryst. Rev. 11 (2005) 21.
[19] R.I. Walton, A. Norquist, R.I. Smith, D. O'Hare, Faraday Discuss. 122 (2003) 331.
[20] A.M. Beale, G. Sankar, Chem. Mater. 15 (2003) 146.
[21] S.D.M. Jacques, O. Leynaud, D. Strusevich, A.M. Beale, G. Sankar, C.M. Martin, P. Barnes (Eds.), Angew. Chem., Int. Ed. 45 (2006) 445.
[22] G. Sankar, T. Okubo, W. Fan, F. Meneau, Faraday Discuss. 136 (2007) 157.
[23] P.P.E.A. de Moor, T.P.M. Beelen, R.A. van Santen, Microp. Mater. 9 (1997) 117.
[24] M.A. Newton, A.J. Dent, J. Evans, Chem. Soc. Rev. 31 (2002) 83.
[25] R. Frahm, B. Griesebock, M. Richwin, D. Lützenkirchen-Hecht, AIP Conf. Proc. 705 (2004) 1411.
[26] A.M. Beale, A.M.J. van der Eerden, S.D.M. Jacques, O. Leynaud, M.G. O'Brien, F. Meneau, S. Nikitenko, W. Bras, B.M. Weckhuysen, J. Am. Chem. Soc. 128 (2006) 12386.
[27] M.A. Newton, C. Belver-Coldeira, A. Martinez-Arias, M. Fernandez-Garcia, Nat. Mater. 6 (2007) 528.
[28] A.M. Beale, A.M.J. van der Eerden, K. Kervinen, M.A. Newton, B.M. Weckhuysen, Chem. Commun. (2005) 3015.
[29] S.J. Tinnemans, J.G. Mesu, K. Kervinen, T. Visser, T.A. Nijhuis, A.M. Beale, D.E. Keller, A.M.J. van der Eerden, B.M. Weckhuysen, Catal. Today 113 (2006) 3.
[30] J.D. Grunwaldt, B.S. Clausen, Top. Catal. 18 (2002) 37.
[31] J.G. Mesu, A.M. Beale, F.M.F. de Groot, B.M. Weckhuysen, J. Phys. Chem. B 110 (2006) 17671.
[32] C.H. Macgillavry, G.D. Rieck, K. Lonsdale (Eds.), International Tables for X-ray Crystallography, vol. III, published for The International Union of Crystallography by The Kynoch Press, Birmingham, 1968, p. 157.
[33] C.T. Chantler, K. Olsen, R.A. Dragoset, J. Chang, A.R. Kishore, S.A. Kotochigova, D.S. Zucker, X-Ray Form Factor, Attenuation and Scattering Tables (version 2.1), National Institute of Standards and Technology, Gaithersburg, MD, 2005, available online: http://physics.nist.gov/ffast (2008, August 29). Originally published as C.T. Chantler, J. Phys. Chem. Ref. Data, 29(4) (2000) 597; C. T. Chantler, J. Phys. Chem. Ref. Data, 24 (1995) 71.
[34] B.S. Clausen, L. Gråbæk, G. Steffensen, P.L. Hansen, H. Topsøe, Catal. Lett. 20 (1993) 23.
[35] I.J. Shannon, F. Rey, G. Sankar, J.M. Thomas, T. Maschmeyer, A.M. Waller, A.E. Palomares, A. Corma, A.J. Dent, G.N. Greaves, J. Chem. Soc., Faraday Trans. 92 (1996) 4331.
[36] G. Meitzner, S.R. Bare, D. Parker, H. Woo, D.A. Fischer, Rev. Sci. Instrum. 69 (1998) 2618.
[37] J.-D. Grunwaldt, S. Hannemann, C.G. Schroer, A. Baiker, J. Phys. Chem. B 110 (2006) 8674.
[38] S.R. Bare, N. Yang, S.D. Kelly, G.E. Mickelson, F.S. Modica, Catal. Today 126 (1–2) (2007) 18.
[39] D. O'Hare, J.S.O. Evans, R.J. Francis, P.S. Halasyamani, P. Norby, J. Hanson, Microp. Mesop. Mater. 21 (1998) 253.
[40] P. Norby, J.C. Hanson, Catal. Today 39 (1998) 301.
[41] http://www.esrf.eu/UsersAndScience/Experiments/XASMS/ID24.
[42] http://www.esrf.eu/UsersAndScience/Experiments/CRG/BM01.
[43] J. Laugier, B. Bochu, Celref software, part of the LMGP Suite using the GETSPEC software referred to by: U.D. Altermatt, I.D. Brown, Acta Crystallogr. A 43 (1987) 125.
[44] J. Rodriguez-Carvajal, FULLPROF: a program for Rietveld refinement and pattern matching analysis, in: Abstr. Satellite Meeting Powder Diffraction, XV Congr. It. Union Cryst., 1990, p. 127.
[45] N. Pernicone, Catal. Today 11 (1991) 85–91.
[46] A.P. Vieira Soares, M.F. Portela, A. Kiennemann, Catal. Rev. Sci. Eng. 47 (2005) 125.
[47] M.R. Antonio, R.G. Teller, D.R. Sandstrom, M. Mehicic, J.F. Brazdil, J. Phys. Chem. 92 (1998) 2939.
[48] O.V. Safonova, M. Tromp, J.A. van Bokhoven, F.M.F. de Groot, J. Evans, J. Phys. Chem. B 110 (2006) 16162.
[49] L. Ehm, S.M. Antao, J.H. Chen, D.R. Locke, F.M. Michel, C.D. Martin, T. Yu, J.B. Parise, S.M. Antao, P.L. Lee, P.J. Chupas, S.D. Shastri, Q.Z. Guo, Powd. Diff. 22 (2007) 108.
[50] A.M. Beale, in: S.D.M. Jacques, J.A. Bergwerff, P. Barnes, B.M. Weckhuysen (Eds.), Angew. Chem. Int. 46 (2007) 8832.